Tuning the Reversible Binding of NO to Iron(II) Aminocarboxylate and Related Complexes in Aqueous Solution

Thorsten Schneppensieper,[a] Stefan Finkler,[a] Almut Czap,[a] Rudi van Eldik,*[a] Martin Heus,[b] Peter Nieuwenhuizen,[b] Carel Wreesmann,[b] and Wiebe Abma[c]

Keywords: Iron / Chelates / Thermodynamics / Nitric oxide / Stability constants

Chelate complexes of Fe^{II} were investigated with respect to their reactivity against nitric oxide and dioxygen. Through a systematic variation of the structure of the polyaminocarboxylate EDTA, a series of 38 potential chelate ligands were selected for Fe^{II}. The nitrosyl complexes were prepared from the Fe^{II} chelates with NO gas and examined spectroscopically by UV/Vis and ATR-IR techniques, and themodynamically by determining the overall binding constants for NO. In addition, the reversibility of NO binding to these Fe^{II} chelates and the rate of the competing oxidation by dioxygen were studied qualitatively. Whereas the studied complexes all form more or less stable nitrosyl complexes with a characteristic band pattern in the UV/Vis spectra and only slightly diverging frequencies for the NO stretching vibration in the IR spectra, they differ considerably in the reversibility of NO binding, the overall NO binding constants and the sensitivity towards dioxygen. It was found that an increasing number of donor groups on the chelate ligand causes a stronger coordination to Fe^{II}, and increases the tendency of the Fe^{II} chelates to transfer electron density from iron to substrates like dioxygen or nitric oxide. This results in an accelerated oxidation of Fe^{II} to Fe^{III} by dioxygen and a more pronounced tendency of the corresponding nitrosyl complexes to slowly decompose to Fe^{III} and N_2O. In addition, the overall binding constant for NO (K_{NO}), which spans a range from $1 \cdot 10^3$ to $2 \cdot 10^7$ M^{-1}, increases in the same direction as a result of the inductive effect of the chelate ligand.

Introduction

Chelate complexes of Fe^{II} in aqueous solution have been suggested as homogeneous catalysts for the selective binding and subsequent reduction of NO to dinitrogen in denitrification processes.[1–9] An essential aspect of this process is the efficient binding of NO by a metal chelate in order to increase its solubility in aqueous solution. Although a number of studies have dealt with the binding of NO to chelate complexes of Fe^{II}, none have undertaken a systematic investigation of the chelate properties in order to optimize the efficiency and reversibility of the binding process.[1,10–14] In this study we undertook a systematic variation of the donor number and donor atoms of multidentate chelates, and determined the overall binding constants for NO to the corresponding Fe^{II} complexes. In addition, we studied the reversibility of the binding process, as well as the UV/Vis and IR spectral changes associated with these reactions. Parallel to this, the competing reaction with dioxygen was also investigated quantitatively. An interesting correlation between the binding ability for NO and the oxygen sensitivity of the Fe^{II} complexes was found. The observed trends are reported in a qualitative way, and the most important factors that control the efficiency and reversibility of the binding of NO to Fe^{II} chelates are discussed.

In order to establish an extended series of chelate ligands that are able to bind NO more or less reversibly in the form of Fe^{II} complexes, we used the polyaminocarboxylate EDTA as a reference and starting point for nearly all structural modifications. The seven-coordinate $[Fe^{II}(EDTA)(H_2O)]^{2-}$ complex[15] certainly belongs to the hitherto best examined systems for NO binding in aqueous solution, and detailed kinetic and thermodynamic data are available in the literature.[16–18] Furthermore, EDTA is an inexpensive industrial product and its structure offers nearly unlimited possibilities for modification. Through a systematic variation of the EDTA structure we obtained a set of altogether 38 chelate ligands summarized in Figure 1. Apart from direct EDTA derivatives (**Series 1**), we also studied a considerable number of MIDA analogues as indirect EDTA derivatives (**Series 2**) in order to investigate the influence of a reduction in the molecular size of the chelate ligand on the NO binding characteristics of the corresponding Fe^{II} complexes.

Since a systematic treatment enables more specific conclusions to be reached on the relation between structure and function of the examined systems, it was advantageous to further divide the EDTA and MIDA analogues in different subgroups. Within the series of EDTA analogues (**Series 1**), the ethylene spacer between the two EDTA nitrogens was varied through branching or elongation (**subgroup a**), or some or all of the four acetic acid end groups were replaced without

[a] Institute for Inorganic Chemistry, University of Erlangen-Nürnberg,
Egerlandstraße 1, 91058 Erlangen, Germany
Fax: (internat.) +49−9131/8527387
E-mail: vaneldik@chemie.uni-erlangen.de
[b] Akzo Nobel Chemical Research Arnhem, Department RPH, P. O. Box 9300, 6800 SB Arnhem, The Netherlands
[c] Paques Bio Systems BV, P.O. Box 52, 8560 AB Balk, The Netherlands

  1434−1948/01/0202−0491 $ 17.50+.50/0

affecting the central ethylenediamine component (**subgroup b**). The MIDA analogues (**Series 2**) are divided into three subgroups. Whereas in **subgroup a** the methyl group of MIDA is exchanged by another non-coordinating group, it is exchanged in **subgroup b** by a further coordinating function. **Subgroup c** summarizes derivatives in which the nitrogen donor of MIDA is replaced by oxygen, sulfur, a methylene group, or an aromatic nitrogen.

Chelate ligands, which cannot be related directly to either MIDA or EDTA analogues, are compiled in a third main group (**Series 3**). These include the phosphonates ATMP, EDTMP, and DTPMP (derivatives of NTA, EDTA, and DTPA), nitrogen-free hydroxycarboxylic acids like TARTRATE and CITRATE, and the aromatic aminocarboxylate APTA.

Results and Discussion

Preliminary Observations

In the following sections, Fe^{II} chelate complexes and the corresponding nitrosyl complexes are indicated by the formulae $[Fe^{II}(L)_x]$ and $[Fe^{II}(L)_x(NO)]$, respectively, where L = chelate ligand. Although the number of bound chelate molecules are only precisely known in a few cases, especially for L = EDTA (x = 1) and MIDA (x = 1 and 2),[19] it is safe to assume that all EDTA analogues form 1:1, and MIDA analogues with three donor groups form either 1:1 or 1:2 complexes with Fe^{II}. In general, the 1:1 complexes are quite stable species in solution as judged from their stability constants reported in the literature.[19] Typical examples are

Series 1: Analogues of EDTA

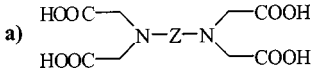

Z = spacer

EDTA: Z = -$(CH_2)_2$-
1,2-PDTA: Z = -$CH(CH_3)$-CH_2-
1,3-PDTA: Z = -$(CH_2)_3$-
HPDTA: Z = -CH_2-$CH(OH)$-CH_2-
1,4-BDTA: Z = -$(CH_2)_4$-
1,6-HDTA: Z = -$(CH_2)_6$-
EGTA: Z = -$(CH_2)_2$-O-$(CH_2)_2$-O-$CH_2)_2$-
CDTA: Z =

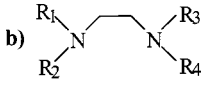

$R_{1\text{-}4}$ = end groups

EDDA: $R_1 = R_3 = H$; $R_2 = R_4 = CH_2$-COOH
α-EDDADP: $R_1 = R_3 = CH_2$-COOH; $R_2 = R_4 = CH(CH_3)$-COOH
β-EDDADP: $R_1 = R_3 = CH_2$-COOH; $R_2 = R_4 = CH_2$-CH_2-COOH
EDTP: $R_1 = R_2 = R_3 = R_4 = CH_2$-$CH_2$-COOH
EDDHPA: $R_1 = R_3 = H$; $R_2 = R_4 = CH(o\text{-}C_6H_4OH)$-COOH
HEDTRA: $R_1 = R_2 = R_3 = CH_2$-COOH; $R_4 = CH_2$-CH_2OH
EDDS: $R_1 = R_3 = H$; $R_2 = R_4 = CH(COOH)$-CH_2-COOH
DTPA: $R_1 = R_2 = R_3 = CH_2$-COOH; $R_4 = (CH_2)_2$-$N(CH_2$-COOH$)_2$

Figure 1. Survey of tested chelate ligands

In order to check these numbers, pH titrations were performed for the complexes $[Fe^{II}(L)_x]$ (L = MIDA, EDTA). Calculations relating to the determination of protonation and complex formation constants were performed using the computer program PSEQUAD.[20] The measured stability constants, $3.39 \cdot 10^{11}$ M^{-2} (L = MIDA) (see Table 1) and $2.29 \cdot 10^{14}$ M^{-1} (L = EDTA) are in good agreement with those reported in the literature.[21] Speciations (see Figure 2) were calculated with the computer program SPECIES.[22] The results for the Fe−MIDA system indicate that below pH 3 no complex formation occurs. Between pH 3 and 5, the 1:1 [Fe(MIDA)] complex is generated, and above pH 5 the 1:2 complex is partially present. At pH 8 the iron is totally complexed and at pH > 10 the 1:2 complex is the dominating species. This species distribution indicates that at pH 5, where most of the experiments were performed, mainly the 1:1 complex will exist. The 1:2 complex will only be present

Series 2: Analogues of MIDA

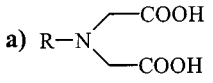

R = non-coordinating group

IDA: R = H
MIDA: R = CH_3
EIDA: R = CH_2-CH_3
^{t}BIDA: R = $C(CH_3)_3$
AIDA: R = C(O)-CH_3
SMIDA: R = CH_2-SO_3H

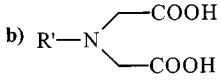

R' = coordinating group

EDG: R' = CH_2-CH_2OH
HPIDA: R' = CH_2-$CH(OH)$-CH_3
NTA: R' = CH_2-COOH
BADA: R' = CH_2-CH_2-COOH
ADA: R' = CH_2-$CONH_2$
CEIDA: R' = CH_2-CH_2-S-CH_2-COOH

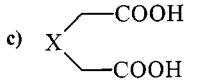

X = hetero atom

ODA: X = O
TDA: X = S
GLUTAR: X = CH_2
DIPIC: X = $N_{arom.}$

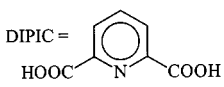

Figure 1. *(Continued)*

Table 1. Stability constants

	log K_1	log K_2	K
$[Fe^{II}(MIDA)_x]$	6.18 ± 0.08	5.35 ± 0.08	$3.39 \cdot 10^{11}$ M^{-2}
$[Fe^{II}(MIDA)_xNO]$	6.86 ± 0.07	4.63 ± 0.09	$3.09 \cdot 10^{11}$ M^{-2}

as the major species when a large excess (ca. 20 fold) of MIDA is used. A similar conclusion was reached on the basis of ^{1}H NMR spectra recorded for the uncoordinated ligand in solution.

Net charges for these complexes are only given when the composition of the complex can be specified, e.g. $[Fe^{II}(EDTA)]^{2-}$. A coordinated water molecule was detected in the crystal structure of the EDTA complex,[15] which can therefore be presented by the formula $[Fe^{II}(EDTA)(H_2O)]^{2-}$. Preliminary water exchange studies on several $[Fe^{II}(L)_x]$ complexes using ^{17}O NMR techniques, indicated that they in general have at least one water molecules bound to the Fe^{II} center.[23] In the absence of further details and for reason of uniformity, water molecules will be omitted in all following formulae. However, it should be kept in mind that some of the complexes are seven-coordinate species, such that the reaction with NO is probably not a simple addition of NO to $[Fe^{II}(L)_x]$ but rather substitution of a labile bound water molecule by NO.

Whereas the coordination stoichiometry of $[Fe^{II}(MIDA)_x]^{(2x-2)-}$ and analogues can now be predicted for the selected experimental conditions in terms of pH and metal to ligand concentration ratio as outlined above, the composition of the corresponding NO complex, viz.

Series 3: Other ligands

ATMP

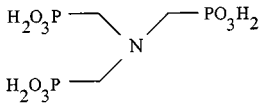

DTPMP

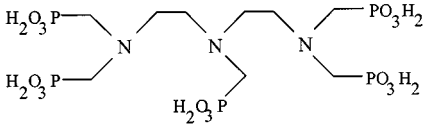

EDTMP

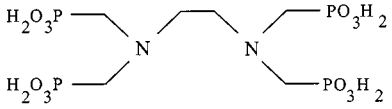

L-TARTRATE

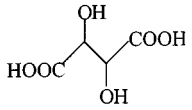

CITRATE

APTA

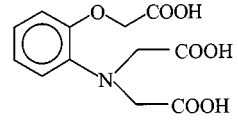

Figure 1. *(Continued)*

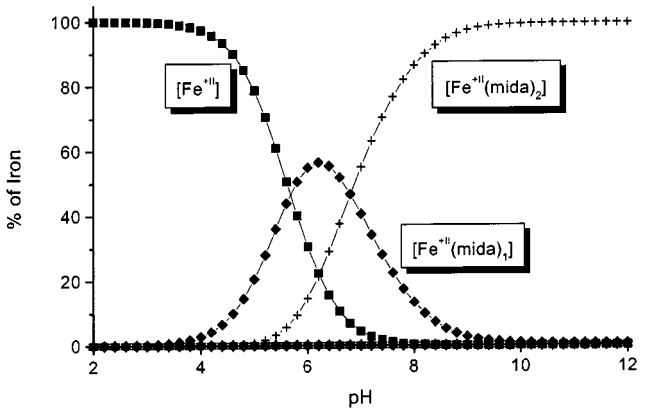

Figure 2. Species distribution curves for the $[Fe^{II}(MIDA)_x]^{(2x-2)-}$ complex [experimental conditions: $[Fe^{II}(MIDA)] = 4 \cdot 10^{-3}$ M, $T = 25$ °C, $I = 0.5$ M ($NaClO_4$)]

$[Fe^{II}(MIDA)_xNO]^{(2x-2)-}$, remains to be determined. For this purpose a potentiometric titration of the NO complex was done. From the speciation diagram it was possible to confirm that under the selected conditions the 1:1 complex is the dominating species in solution (see Figure 3).

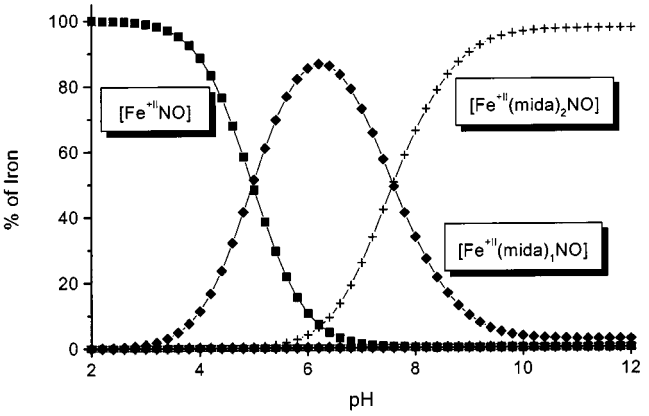

Figure 3. Species distribution curves for the $[Fe^{II}(MIDA)_xNO]^{(2x-2)-}$ complex [experimental conditions: $[Fe^{II}(MIDA)NO] = 4 \cdot 10^{-3}$ M, $T = 25$ °C, $I = 0.5$ M ($NaClO_4$)]

pH titrations of the $[Fe^{II}(MIDA)_xNO]$ complex resulted in a stability constant of $3.09 \cdot 10^{11}$ M^{-2} (Table 1) and show that there is nearly no change in the overall stability constant between $[Fe^{II}(MIDA)_x]$ and $[Fe^{II}(MIDA)_xNO]$. The addition of NO caused a small but significant change in the logK_1 and logK_2 values in favor of the 1:1 complex.

The species distribution (Figure 3) clearly indicates that the reaction with NO significantly stabilizes the 1:1 complex in a manner that at pH 5 more of the 1:1 [Fe(MIDA)NO] complex is generated than found for the speciation in the absence of NO. In fact, the increase in the 1:1 complex is approximately twice the decrease in the 1:2 complex concentration during the introduction of NO into the solution.

It can be concluded from the above described experiments that MIDA and analogous chelates mainly form 1:1 complexes with Fe^{II} and NO. $[Fe(MIDA)_2NO]^{2-}$ can only be prepared in solution in the presence of a large, at least 20 fold, excess of MIDA.

General Features in the UV/Vis and ATR-IR Spectra of Fe^{II} Nitrosyl Complexes

UV/Vis spectra

The identification and spectral characterization of metal−NO complexes has received much attention from researchers over the last few decades, and the results are summarized in some selected publications.[10,11,16,24−27] In the majority of cases, especially when the chelate ligand L is a polyaminocarboxylate, the UV/Vis spectra of the nitrosyl complexes $[Fe^{II}(L)_x(NO)]$ are characterized by three absorption bands: two strong *charge-transfer (C-T)* bands around 340 and 440 nm, respectively, and one weaker *d-d* band between 580 and 640 nm (data are summarized in Table 2). Whereas the position of the high energy *C-T* band at about 340 nm is almost not affected by the nature of the bound chelate ligand, the low energy *C-T* band around 440 nm shows a small, and the *d-d* band a strong dependence on the selected chelate. In addition, a correlation exists between the positions of the *C-T* and *d-d* bands: with decreasing wavelength of the low energy *C-T* band, the wavelength of the *d-d* band increases (see Figure 4).

The two extreme cases are on the one hand the non-chelated iron complex, $[Fe^{II}(H_2O)_5(NO)]^{2+}$, with absorption bands at 451 nm and 585 nm (similar values were also found in the presence of potential ligands such as ^{t}BIDA, EDTP, and glutaric acid which do not coordinate efficiently to Fe^{II}), and on the other hand complexes with coordinated EDTA, DTPA, or HEDTRA, which have absorption bands at about 434 ± 1 nm and 635 ± 2 nm. Most of the other nitrosyl complexes exhibit an intermediate position with respect to their UV/Vis spectra.

Some preliminary observations led us to believe that the shift in the C-T band to lower and that of the *d-d* band to higher wavelengths may be associated with a systematic displacement of electron density between the iron metal center and NO. This is particularly indicated by the chemical features of the corresponding $[Fe^{II}(L)_x]$ complexes

Table 2. Survey of UV/Vis data, IR data, and Stability constants K_{NO} for $[Fe^{II}(L)_x(NO)]$ complexes with different chelate ligands L

Ligand	Fe^{II}/Lig.[a]	K_{NO} values [M^{-1}][b] with exp. errors	UV data [nm][b]	IR data [cm^{-1}][c]
H_2O		(1.15 ± 0.05) ×10^3	336 (440), **451** (265), **585** (85)	**1810** (pH 3.1)
edta	1:1.25	(2.05 ± 0.15) ×10^6	342 (1080), **435** (820), **633** (130)	**1777** (pH 4.2)
cdta	1:1	-	**430**, **628**	**1774** (pH 3.7)
1.2-pdta	1:1.25	(7.4 ± 0.6) ×10^5	343 (1130), **436** (860), **628** (140)	**1775** (pH 4.7)
1,3-pdta	1:1.2	(1.4 ± 0.3) ×10^4	343 (1065), **446** (845), **621** (135)	**1762** (pH 4.7)
hpdta	1:1.25	(1.1 ± 0.2) ×10^5	336 (1050), **437** (740), **619** (160)	**1792** (pH 5.0)
1,4-bdta	1:1.2	(3.75 ± 0.05) ×10^3	340 (980), **444** (650), **598.5** (135)	**1784** (pH 4.3)
1,6-hdta	1:1.1	(7.6 ± 0.4) ×10^3	340 (970), **443** (640), **597** (130)	**1783** (pH 5.4)
egta	1:1.25	(7.7 ± 0.6) ×10^3	341 (1120), **440** (680), **613** (130)	**1783** and **1802** (pH 5.4)
edda	1:1.25	(3.3 ± 0.5) ×10^5	341 (975), **437** (920), **620** (135)	**1765** (pH 5.7)
α-eddadp	1:1	-	**430**, **626**	**1781** (pH 3.5)
β-eddadp	1:1.1	(8.6 ± 0.4) ×10^5	346 (1065), **443** (950), **628** (140)	**1764** (pH 4.9)
edtp	1:1.5	(1.4 ± 0.1) ×10^3	337 (620), **452** (400), **580 s** (105)	**1755** (pH 6.3)
eddhpa	1:1.25, pH = 8.0	> 1 × 10^7	**442** (2450)	not soluble
hedtra	1:1.25	(1.5 ± 0.2) ×10^7	344 (1080), **434** (815), **634** (130)	**1777** (pH 5.0)
(*s,s*)-edds	1:1.3	(9.0 ± 1.0) ×10^5	345 (955),**439**(960), **638** (135)	**1766** (pH 4.5)
rac-edds	1:1.3	(1.9 ± 0.2) ×10^6	344.5 (950), **439** (975), **635** (135)	**1765** (pH 4.8)
dtpa	1:1.25	(3.0 ± 0.3) ×10^6	344 (1200), **433** (830), **636** (130)	**1778** (pH 5.5)
ida	1:3	(1.2 ± 0.1) ×10^4	339 (1050), **440** (815), **604** (140)	**1769** (pH 7.3)
mida	1:3	(9.5 ± 0.7) ×10^3	341 (1065), **444** (740), **598** (145)	**1777** (pH 6.4) **1783** (pH 4.9)
eida	1:3	(7.6 ± 0.3) ×10^3	340 (1020), **443.5** (640), **596.5** (130)	**1783** (pH 7.9)
^{t}bida	1:3	(1.30 ± 0.05) ×10^3	337 (605), **448.5** (360), **584.5** (110)	**1809** (pH 4.2)
aida	1:3	(4.3 ± 0.2) ×10^3	338 (775), **443** (540), **594** (115)	**1810** (pH 3.4)
smida	1:3	(1.1 ± 0.2) ×10^4	339 (1005), **440.5** (800), **605** (140)	**1779** (pH 7.1)
edg	1:3	(1.6 ± 0.2) ×10^5	340 (1230), **437** (810), **610.5** (135)	**1762** (pH 9.2)
hpida	1:3	(2.4 ± 0.2) ×10^5	341 (1250), **436** (835), **614** (140)	**1798** and **1763** (pH 8.6)
nta	1:2.5	(1.75 ± 0.15) ×10^6	342 (1230), **439** (870), **600** (150)	**1793** (pH 6.9)
bada	1:2.5	(4.7 ± 0.4) ×10^5	343.5 (1295), **446** (930), **612** (150)	**1782** (pH 5.4)
ada	1:3	(5.15 ± 0.15) ×10^5	342.5 (1270), **439** (780), **593** (150)	**1801** (pH 8.0)
ceida	1:1.3	(1.2 ± 0.3) ×10^6	**432** (730), **624** (125)	**1791** (pH 4.2)
glutaric acid	1:4	(1.1 ± 0.1) ×10^3	335 (470), **450.5** (290), **584** (95)	
oda	1:3	(4.6 ± 0.1) ×10^3	337 (815), **446.5** (500), **537 s** (210)	not soluble
tda	1:3	(2.1 ± 0.1) ×10^3	340.5 (980), **451** (480), **575 s** (140)	not soluble
dipic	1:1	(1.1 ± 0.1) ×10^4	338 (1170), **433** (880), **600** (160)	not soluble
dipic	1:2.2	not determined	336 (860), **446** (990)	not soluble
atmp	1:3.0	(1.4 ± 0.2) ×10^6	344 (1470), **452** (790), **585** (190)	
edtmp	1:1.5	(1.3 ± 0.2) ×10^6	345 (1320), **444.5** (695), **602** (130)	
dtpmp	1:1.5	(1.35 ± 0.15) ×10^6	346 (1250), **451** (670), **578 s** (175)	
L-tartrate	1:2.5	(1.3 ± 0.1) ×10^3	336 (815), **444** (375), **567** (110)	
citrate	1:2.3	(2.1 ± 0.3) ×10^4	338 (1120), **443** (710), **575** (175)	
apta	1:1.3	(4.5 ± 0.2) ×10^4	344 (950), **444** (600), **542** (240)	**1795** (pH 6.5)

[a] Fe^{II}/Lig. indicates the ratio beween Fe^{II} and chelate ligand L which was used to prepare the $[Fe^{II}(L)_x(NO)]$ complexes for UV/Vis spectra and determination of K_{NO} values. − [b] Conditions (*if not otherwise indicated*): 1 mM Fe^{II} ($FeSO_4$); 100 mM acetic acid/acetate buffer, pH = 5.0; I = 0.5 (adjusted with $NaClO_4$); $T \approx 23$ °C; molar extinction coefficients are quoted in brackets in M^{-1} cm^{-1}. − [c] Conditions (only for IR): 200 mM Fe^{II}; excess of chelate ligand L: 10 to 25%; unbuffered solutions.

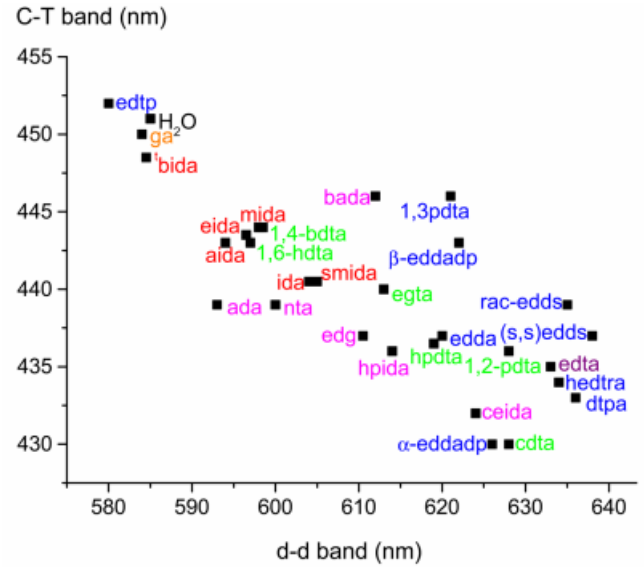

Figure 4. Correlation between the *C-T* and *d-d* band positions in the UV/Vis spectra of $[Fe^{II}(L)_x(NO)]$ complexes with L = polyaminecarboxylates.

which show, as described in detail below, in the direction from L = H_2O to L = EDTA, HEDTRA, or DTPA an increase in oxygen sensitivity accompanied by a decrease in the reversibility of the binding of NO·. Along these lines it could be favorable to consider the pentaaqua and MIDA nitrosyl complexes formally as $[Fe^{II}(H_2O)_5(NO^{\cdot})]^{2+}$ and $[Fe^{II}(MIDA)(NO^{\cdot})]$, respectively, compared to the EDTA nitrosyl complex as $[Fe^{III}(EDTA)(NO^{-})]^{2-}$.[27,28] This would indicate that in the former case the bound NO has more a radical, whereas in the latter case NO has more an anionic character. However, in the selected systems the difference in the distribution of electron density between Fe^{II} and NO seems to be very small, which is most evident from the ATR-IR spectra discussed in the following section.

Fe^{II} nitrosyl complexes which deviate in their UV/Vis data from the common features described above, were in general formed by chelate ligands other than polyaminocarboxylates (Figure 1, **Series 2 subgroup c** and **Series 3**). The most pronounced deviation in the UV/Vis spectrum is exhibited by the Fe^{II} complex of DIPIC. In contrast to all other studied $[Fe^{II}(L)_x]$ complexes, the complexes with L = DIPIC show strong bands associated with the aromatic ring at 459 nm (x = 1) or 482 nm (x = 2). Recently, several structures of iron(II/III) complexes with DIPIC have been reported, and structures with different stoichiometries could be characterized.[29−32] Even the seven-coordinate complex $[Fe^{II}(DIPIC)_2H_2O]^{2-}$ was characterized, which underlines our assumption that in the 1:2 complexes a water molecule can be coordinated in the seventh position.[31]

ATR-IR Spectroscopy

IR spectroscopy is considered to be an useful tool for the determination of the binding mode and oxidation state of NO in metal based complexes.[25,33] Efforts to distinguish between NO bound to the metal center in a linear mode as NO^+ or in a bent mode as NO^- on the basis of the NO stretching frequencies, revealed a considerable overlap in the range between 1600 and 1800 cm^{-1}.[33−35] It seems that there is a gradual change from the extreme NO^- form at lower frequency to the extreme NO^+ form at higher values. On this basis, changes in the electron delocalization for different $Fe^{II}(L)-NO$ complexes should be accompanied by characteristic shifts in the NO stretching frequencies.

Since only a few IR spectra of polyaminocarboxylate−Fe−NO complexes are known from the literature,[18] an extended series of $[Fe^{II}(L)_x]$ and $[Fe^{II}(L)_x(NO)]$ complexes were investigated by IR spectroscopy using the ATR technique.[36] The series was limited to those complexes which could be synthesized at a concentration level required to produce undistorted spectra with a satisfactory intensity and resolution (see Table 2). The values for example, obtained for $[Fe^{II}(EDTA)]^{2-}$ and $[Fe^{II}(EDTA)(NO)]^{2-}$, viz. ν(COO⁻, asym.) = 1588 cm^{-1}, ν(COO⁻, sym.) = 1406, 1325 cm^{-1}, and ν(COO⁻, asym.) = 1611 cm^{-1}, ν(COO⁻, sym.) = 1398, 1317 cm^{-1}, ν(NO) = 1777 cm^{-1}, respectively, are in good agreement with literature data.[37]

In the series of the complexes $[Fe^{II}(H_2O)_5(NO)]^{2+}$, $[Fe^{II}(MIDA)(NO)]$, and $[Fe^{II}(EDTA)(NO)]^{2-}$, the shift in the NO band from 1810 to 1783 to 1777 cm^{-1}, respectively, could suggest a gradual change from a partially more positive (NO^+) to a partially more negative (NO^-) binding character of NO. However, the frequencies of the NO vibrations for the MIDA and EDTA complexes hardly differ from each other, with the result that the deviation is too small to predict a significantly different binding mode. It follows that although the reported IR data do not reveal detailed information on the nature of the Fe-NO bond, the spectra do supplement the UV/Vis data and provide direct evidence for the reversible coordination of NO to the Fe^{II} centers.

Qualitative Characteristics of Fe^{II}-L Complexes During the Reactions with NO and O_2

The influence of the chelate ligand on the chemical features of the Fe^{II} complexes is clearly reflected by the reversibility of NO binding and the oxidation rate of $[Fe^{II}(L)_x]$. There are two extreme cases in which way both substrates (O_2 and NO) react with Fe^{II} chelates: in the first case they bind reversibly to the Fe^{II} center, whereas in the second case a shift of electron density from iron to the substrate, accompanied by the irreversible formation of the corresponding Fe^{III} complex, occurs. These opposite cases are illustrated on the one hand by iron complexes of water (aqua complexes) or several MIDA analogues (reversible substrate binding), and on the other hand by iron complexes of several EDTA analogues (irreversible substrate binding). In the following, MIDA and EDTA were selected as typical chelate ligands in order to examine the opposite features of both groups of complexes in more detail.

Reversibility of the Binding of NO to $[Fe^{II}(L)_x]$ Complexes

The main characteristic of $[Fe^{II}(MIDA)]$ is its ability to bind NO completely reversibly.

This is evident from the UV/Vis spectra in Figure 5, which show the mutual conversion between the $[Fe^{II}(MIDA)]$ complex (traces a, c, and e) and the corresponding nitrosyl complex $[Fe^{II}(MIDA)(NO)]$ (traces b, d, and f) by bubbling alternately NO or an inert gas through the complex solution. Obviously, the inert gases remove low concentrations of free NO from the solution, which are formed by a partial dissociation of the nitrosyl complex. In this way the equilibrium is driven back to the left side of Equation (1) to regenerate finally the pure starting complex $[Fe^{II}(MIDA)]$, from which the nitrosyl complex can be formed again.

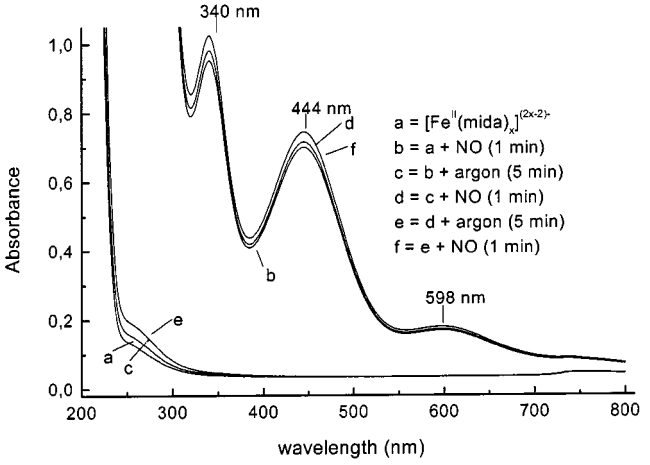

Figure 5. Reversibility of the NO binding to $[Fe^{II}(MIDA)]$ (exp. conditions: 1 mM $FeSO_4 \cdot 7\ H_2O$; 2.5 mM MIDA; 100 mM acetate buffer; pH = 5.0; T = 23 °C)

$$[Fe^{II}(MIDA)] + NO \rightleftharpoons [Fe^{II}(MIDA)(NO^{\cdot})] \quad (1)$$

The complete reversibility of the binding of NO to $[Fe^{II}(MIDA)]$ indicates that practically no electron transfer between Fe^{II} and NO occurs, which means that NO is presumably bound as radical to the Fe^{II} center. A similar behavior was found for the ligand free system (i.e. $[Fe^{II}(H_2O)_6]^{2+}$ species) and in the case of all MIDA analogues which are compiled in Figure 1, **Series 2** under **subgroups a** and **c**.

In comparison to the analogous MIDA complex, the NO chemistry of $[Fe^{II}(EDTA)]^{2-}$ is somewhat more complex.[16–18] As shown in Figure 6, there is to a certain extent a reversible binding of NO to $[Fe^{II}(EDTA)]^{2-}$ that can be observed when the whole experiment is performed within a time period of less than one hour. The fact that from the partially decomposed nitrosyl complex (trace d) the initial nitrosyl complex (trace e) can be restored completely, indicates that no irreversible electron transfer from Fe^{II} to NO occurred during the release of NO. Obviously, an equilibrium between $[Fe^{II}(EDTA)]^{2-}$ and the corresponding nitrosyl complex must exist [Equation (2)], which differs from the corresponding equilibrium for the MIDA system [see Equation (1)] only with respect to the position of the equilibrium, which lies more on the right side and leads to the observed poorer release of NO from the complex (Figure 6, traces c and d).

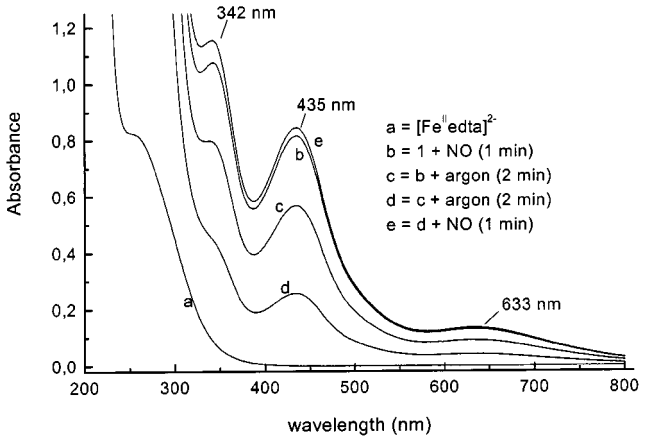

Figure 6. Reversibility of the NO binding to $[Fe^{II}(EDTA)]^{2-}$ (exp. conditions: 1 mM $FeSO_4 \cdot 7\ H_2O$; 1.25 mM EDTA; 100 mM acetate buffer; pH = 5.0; 23 °C)

$$[Fe^{II}(EDTA)]^{2-} + NO \rightleftharpoons [Fe^{II}(EDTA)(NO)]^{2-} \quad (2)$$

An irreversible electron transfer from Fe^{II} to NO occurs in the case of the EDTA system on a time scale of several hours, which is followed by the dissociation of the complex according to Equation (3) into $[Fe^{III}(EDTA)]^{-}$ and NO^{-} (nitroxyl anion). $[Fe^{III}(EDTA)]^{-}$ is identified in the UV/Vis spectrum (Figure 6) by its very intense absorption band below 400 nm,[38] whereas the unstable nitroxyl anion reacts immediately to nitrous oxide (N_2O). The latter product was detected mass spectrometrically in the form of N_2O in the gas phase.[39] As shown in Figure 7, the predominant part of $[Fe^{II}(EDTA)(NO)]^{2-}$ decomposes at room temperature within about 20 h.

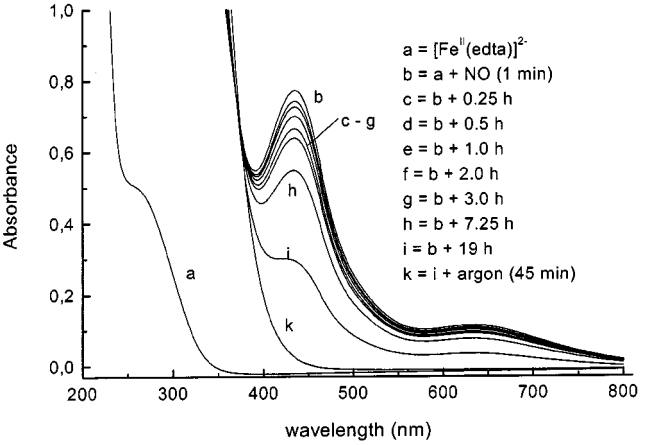

Figure 7. Thermal decomposition of $[Fe^{II}(EDTA)(NO)]^{2-}$ to $[Fe^{III}(EDTA)]^{-}$ and N_2O (exp. conditions: 1 mM $FeSO_4 \cdot 7\ H_2O$; 1 mM EDTA; 100 mM acetate buffer; pH = 5.0; T = 23 °C)

$$[Fe^{II}(EDTA)(NO)]^{2-} \xrightarrow{slow} \underset{(unstable)}{\{Fe^{III}(EDTA)(NO^{-})\}^{2-}} \rightarrow [Fe^{III}(EDTA)]^{-} + \underset{(unstable)}{\{NO^{-}\}} \quad (3)$$

In summary, for the $[Fe^{II}(EDTA)]^{2-}$/NO system a rapid equilibrium between $[Fe^{II}(EDTA)]^{2-}$ and $[Fe^{II}(EDTA)(NO)]^{2-}$

exists, which is followed by a slow and irreversible redox process accompanied by the dissociation of the complex to form $[Fe^{III}(EDTA)]^-$ and N_2O. The slow electron transfer process can be considerably accelerated when instead of EDTA, CDTA, or α-EDDADP are used as chelating ligands. In these cases the dissociation of the nitrosyl complexes to $[Fe^{III}(L)]^-$ and N_2O occurs on a time scale of some minutes. Obviously, small steric and electronic effects may control in a very sensitive way the rate of this irreversible electron transfer process.

Oxygen Sensitivity of $[Fe^{II}(L)_x]$ Complexes

In analogy to the reaction of $[Fe^{II}(MIDA)]$ with nitric oxide, the chemical behavior in the presence of air oxygen indicates that almost no electron transfer reaction from Fe^{II} to O_2 occurs. Consequently, solutions of $[Fe^{II}(MIDA)]$ are not oxidized to $[Fe^{III}(MIDA)]^+$ by air [Equation (4)].

$$[Fe^{II}(MIDA)] + O_2 \not\longrightarrow [Fe^{III}(MIDA)]^+ \quad (4)$$

In contrast to this, $[Fe^{II}(EDTA)]^{2-}$ is highly oxygen sensitive. Its transformation to the corresponding $[Fe^{III}(EDTA)]^-$ complex [Equation (5)] is complete in less than 1 minute. This oxidation reaction proceeds according to a complex multistep mechanism which was extensively studied in the literature.[40−43]

$$2\,[Fe^{II}(EDTA)]^{2-} + {}^1/_2\,O_2 + 2\,H^+ \xrightarrow{\text{fast}} 2\,[Fe^{III}(EDTA)]^- + H_2O \quad (5)$$

Besides EDTA, a similarly high oxidation rate of Fe^{II} complexes is observed when the EDTA analogues 1,2-PDTA, CDTA, HEDTRA, EDDS, and α-EDDADP are used (see Figure 1, **Series 1**).

Comparison Between the Fe^{II} Complexes of MIDA and EDTA Analogues

A final comparison between the MIDA system, and the EDTA, CDTA, and α-EDDADP systems, show that the $[Fe^{II}(MIDA)]$ complex can reversibly bind NO and probably also O_2, but does not tend to undergo any electron transfer process, neither to NO, nor to O_2. In contrast, Fe^{II} complexes of the above mentioned EDTA analogues undergo electron transfer processes both to O_2 and NO. The final products of these reactions are $[Fe^{III}(L)]^-$ and either H_2O or N_2O. Whereas the electron transfer from $[Fe^{II}(L)]^{2-}$ to dioxygen is always very fast, the redox reaction with NO is much slower, especially in the case of EDTA.

Stability Constants (K_{NO}) for $[Fe^{II}(L)_x(NO)]$ Complexes

Measurement of the K_{NO} Values

Stability constants for nitrosyl complexes are based on the equilibrium between $[Fe^{II}(L)_x]$ and $[Fe^{II}(L)_x(NO)]$ complexes [Equation (6)] and are therefore defined by Equation (7).

$$[Fe^{II}(L)_x] + NO \underset{k_{off}}{\overset{k_{on}}{\rightleftharpoons}} [Fe^{II}(L)_x(NO)] \quad (6)$$

$$K_{NO} = k_{on} / k_{off} = \frac{[Fe^{II}(L)_x(NO)]}{[Fe^{II}(L)_x]\cdot[NO]} \quad (7)$$

In general, quite vague and rather divergent K_{NO} data for only a few Fe^{II}−polyamino−carboxylate complexes exist in the literature, especially for the chelating ligands EDTA, NTA, and DTPA and for aquated Fe^{II}, $[Fe^{II}(H_2O)_5(NO)]^{2+}$. A comprehensive survey of literature data is given in the review of Demmink et al.[16] These data were often determined indirectly, e.g. from kinetic measurements according to the relationship $K_{NO} = k_{on}/k_{off}$. The disadvantage of such indirect methods is especially the low degree of accuracy of the calculated values.

In our work, we successfully adopted a direct approach to obtain the equilibrium constant K_{NO} by utilizing the recently developed possibility to measure the concentration of free NO in solution with a NO electrode.[44] The remaining unknown equilibrium concentrations in Equation (7), viz. $[Fe^{II}(L)_x(NO)]$ and $[Fe^{II}(L)_x]$, could be easily determined by UV/Vis spectroscopy.

Influence of the Chelate Ligands on the Magnitude of the K_{NO} Values

The K_{NO} values for the $[Fe^{II}(L)_x(NO)]$ complexes are summarized on a logarithmic scale in Figure 8**a**, in which the different groups and subgroups of chelate ligands are presented in different colors (the corresponding numerical K_{NO} values with their relative error limits are given in Table 2). The scale in Figure 8**a** extends a range from $1\cdot10^3$ M^{-1} to $2\cdot10^7$ M^{-1}. In general, coordination of a chelate ligand to Fe^{II} considerably stabilizes the NO binding on the complex.

A detailed analysis of the magnitude of K_{NO} as a function of the chemical structure of the chelate ligand suggests that both electronic and steric effects have a pronounced influence. The highest K_{NO} values are found for ligands such as EDTA, DTPA, HEDTRA, EDDS, EDTMP, NTA, CEIDA, and ATMP, which have at least four strong donor groups and can bind effectively to the Fe^{II} center. A reduction in the number of strong chelating groups as well as an increased steric hindrance, or elongation of the distances between the chelate groups, lead to a remarkable decrease in the K_{NO} values.

Figure 9 shows a correlation between the K_{NO} values and the position of the *C-T* band for nearly the complete series of nitrosyl complexes. The shift in the *C-T* band to lower wavelengths is probably caused by a more pronounced ligand to metal charge transfer from NO to Fe. The synchronous increase in the band energy and the K_{NO} values in Figure 9 indicates that charge transfer seems to play an important role in the stabilization of the Fe−NO bond. For the very stable $[Fe(EDTA)NO]^{2-}$ complex, the Fe−NO bond is suggested to have significant $Fe^{III}-NO^-$ character and the *LMCT* band occurs at 435 nm, i.e. it has a high energy barrier. On the other hand, for the less stable $[Fe(H_2O)_5(NO)]^{2+}$ complex the *LMCT* band occurs at significantly lower energy (451 nm), with the result that the Fe−NO bond is suggested to have more of a $Fe^{II}-NO$

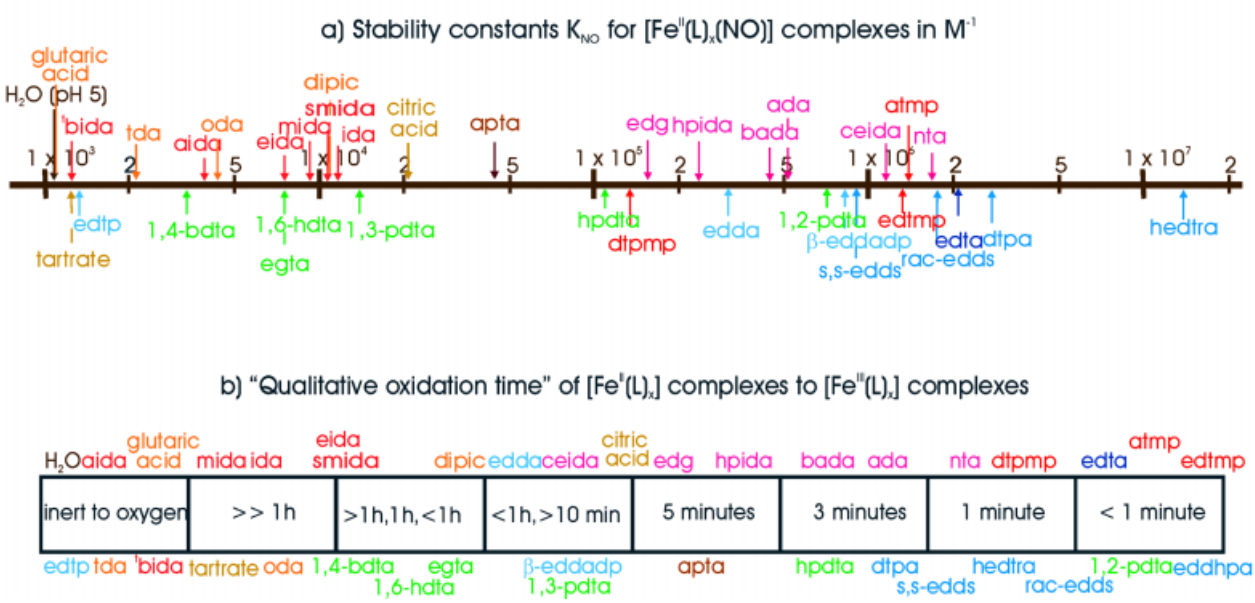

Figure 8. Correlation between K_{NO} and qualitative oxidation time of $[Fe^{II}(L)_x]$ complexes

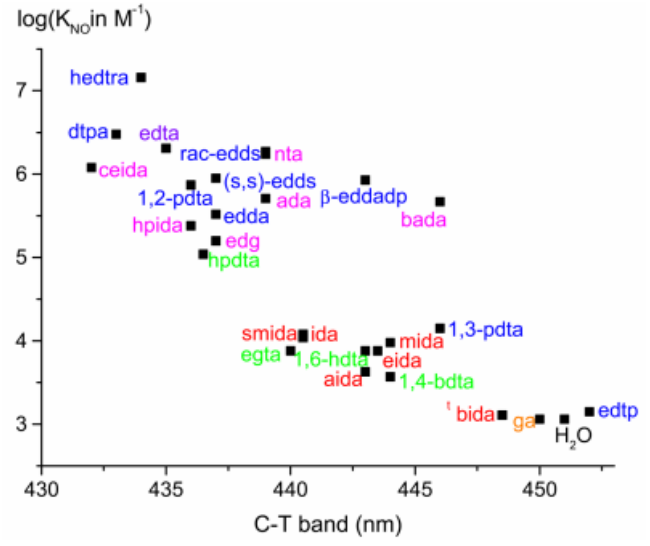

Figure 9. Correlation between the logarithmic K_{NO} values and the position of the *C-T* band in the UV/Vis spectra of $[Fe^{II}(L)_x(NO)]$ complexes with L = polyaminecarboxylates

character. Thus the position of the *LMCT* band is a measure of the charge distribution in the Fe−NO band and correlates directly with the stability of the Fe(L)NO complex.

Following this more general interpretation of the influence of the chelate ligand on the magnitude of K_{NO}, different types of ligands are discussed in more detail.

Stability Constants of $[Fe^{II}(L)(NO)]$ Complexes for EDTA Analogues

For the stability constant of the EDTA complex, $[Fe^{II}(EDTA)(NO)]^{2-}$, a value of approx. $2{\cdot}10^6$ M^{-1} was found, which lies far on the right end of the scale in Figure 8**a** and is in good agreement with literature data ranging between $1.5{\cdot}10^6$ and $3{\cdot}10^6$ M^{-1} at 20 to 25 °C.[14] The high formation constant of the EDTA complex is probably caused by the tailor-made structure of EDTA, which tightly binds all six donor groups to the Fe^{II} center forming five sterically favored five-member rings.

The tuning of the EDTA structure as outlined in Figure 1, **Series 1** (indicated by blue and green colours in Figure 8**a**), clearly demonstrates that the formation of such five-member rings between the donor groups of the ligand and the Fe^{II} center is the most crucial factor for the stabilization of the Fe^{II}−NO bond in the complex. Whereas in 1,2-PDTA the branching of the ethylene spacer of EDTA by a methyl group has only a quite minor influence on the K_{NO} value, both the elongation of the ethylene spacer in the ligands 1,3-PDTA, 1,4-BDTA, 1,6-HDTA, and EGTA, and the substitution of all acetate groups in EDTP by propionate cause a drastic decrease or even a complete loss in the tendency of the ligand to bind to the iron center. This is reflected by K_{NO} values that shift more and more to the value for the pentaaqua nitrosyl complex on the left end of the scale in Figure 8**a**. Obviously, the formation of higher than five-member chelate rings on Fe^{II} is very unfavorable. Therefore, it is not surprising that EDTP with its four elongated carboxylate arms completely looses its binding ability, whilst in 1,3-PDTA, 1,4-BDTA, 1,6-HDTA, and EGTA a coordination of one of both the aminodiacetate units of the ligand to Fe^{II} should still be possible. The exceptional position of the K_{NO} value for the HPDTA complex, which is about ten-fold higher than the value for the 1,3-PDTA complex, is probably caused by coordination of the hydroxyl group to the iron center.

In comparison to the above mentioned ligands, a less pronounced reduction in the K_{NO} constants was observed when only two acetate groups of EDTA were either omitted (EDDA) or substituted by propionate (β-EDDADP) groups. This indicates that in the EDTA structure, besides the ethylene spacer, only two of the four acetate groups are most essential to stabilize the binding of NO. In addition, the deviations between the K_{NO} values of the EDDA and β-ED-

DADP complexes suggest that the propionate groups do not completely loose their ability to bind to Fe^{II}.

The Fe^{II} complexes of EDDS and DTPA have similar K_{NO} values as the EDTA complex, indicating that neither the substitution of the four acetate groups by two succinate groups (EDDS) nor the elongation of the system by an additional ethyleneaminediacetate unit (DTPA) considerably affect the binding characteristics. From the three possible stereoisomers of EDDS, the (*s*,*s*)-form, a natural product synthesized by *Amycolatopsis orientalis*,[45] shows a two-fold lower K_{NO} value than the optical inactive "racemate". It is reasonable to expect that the content of the *meso*-form in the racemate is responsible for the higher K_{NO} value.

Among the EDTA analogues, HEDTRA forms a nitrosyl complex with the highest stability constant. K_{NO} ($1.45 \cdot 10^7$ M^{-1}) exceeds more than five times the value for the EDTA complex. It is not easy to account for this high value, since the molecular structure of the HEDTRA complex is unknown in solution. Probably the hydroxyl group is not (or only weakly) coordinated to the metal center, such that the change in geometry of the complex enhances the stability of the $Fe^{II}-NO$ bond. This suggestion is supported by preliminary kinetic data, which indicate that especially the dissociation rate of NO from the complex (k_{off}) is much slower than in the case of the EDTA complex.[46]

Stability Constants of $[Fe^{II}(L)_x(NO)]$ Complexes for MIDA Analogues

In comparision to $[Fe^{II}(H_2O)_5(NO)]^{2+}$, complexes of MIDA and other three-dentate MIDA analogues stabilize the binding of NO only by a maximum factor of 10, i.e. the K_{NO} values hardly exceed 10^4 M^{-1} (Figure 8**a**, red and orange colors). Under the assumption that, as it was shown in the case of L = MIDA, these ligands selectively form 1:1 nitrosyl complexes with Fe^{II}, the at least 200 times lower stabilization of the $Fe^{II}-NO$ bond in comparison to the EDTA complex can be accounted for in terms of the different coordination geometry of the donor groups. The crystal structure of $[Fe^{II}(EDTA)H_2O]^{2-}$ shows a labile coordinated water molecule as a seventh donor group which is bound nearly opposite to both nitrogens of the mono-capped trigonal-prismatic structure.[15] In the nitrosyl complex, NO most probably substitutes the labile water molecule and as a consequence the $Fe^{II}-NO$ bond is considerably polarized by the strong inductive effect of both opposite nitrogens, and therefore has a high stability.

For the series of three-dentate MIDA analogues, the lower stabilization of the $Fe^{II}-NO$ bond by coordinated ODA, TDA, and AIDA is obviously due to a reduced donor capacity of either the hetero atoms, oxygen (ODA) and sulfur (TDA), or the nitrogen lone pair of AIDA which is delocalized by the acetyl group.

Four-dentate MIDA analogues, which have an additional coordinating group bound to the IDA nitrogen (Figure 1, **Series 2**, **subgroup b**), show in comparison to the three-dentate ligands a strong increase in the K_{NO} values (Figure 8**a**, pink colour). Whereas a hydroxyl group (EDG, HPIDA) increases the stability constant by a factor of about 20, a third carboxylate group (NTA, BADA, CEIDA) can cause a larger than 100 fold enhancement. The most pronounced effect was found in the case of NTA ($K_{NO} = 1.75 \cdot 10^6$ M^{-1}), which likely coordinates to the iron center by creating three sterically favoured five-membered rings. As shown before, both the elongation of an acetate to a propionate group (BADA) and the amide delocalization of ADA, lower the ability to coordinate NO to Fe^{II} and decrease the K_{NO} value by a factor of about 3 in comparison to the NTA complex. The high K_{NO} value of the CEIDA complex ($1.2 \cdot 10^6$ M^{-1}) is probably caused by the fact that the third ligand arm of this chelate coordinates to the Fe^{II} center with both the sulfur and the carboxylate group by forming two five-member rings.

Stability Constants of $[Fe^{II}(L)_x(NO)]$ Complexes for L ≠ Polyaminocarboxylates

The phosphonates ATMP, EDTMP, and DTPMP represent derivatives of the polyaminocarboxylates NTA, EDTA, and DTPA, in which the carboxylate groups are substituted by phosphonate groups. Although the positions of the absorption bands in the UV/Vis spectra differ considerably for the $Fe^{II}-NO$ complexes of both groups (Table 2), the K_{NO} values are in the case of ATMP and EDTMP amazingly similar to the constants for the corresponding NTA and EDTA complexes. This demonstrates that phosphonate is comparable to carboxylate in coordinating to Fe^{II} and stabilizing the $Fe^{II}-NO$ bond. Of both the nitrogen-free compounds, L-tartrate and citrate, only citrate binds strongly to Fe^{II} and causes in comparison to $[Fe^{II}(H_2O)_5(NO)]^{2+}$ a considerably enhanced stability of the Fe^{II}-NO bond with a value of about $2 \cdot 10^4$ M^{-1}.

Correlation Between the Oxygen Sensitivity of $[Fe^{II}(L)_x]$ and the Stability Constants of the Corresponding Nitrosyl Complexes

By comparing the oxygen sensitivity of the $[Fe^{II}(L)_x]$ complexes with the stability constants of the nitrosyl complexes, an interesting correlation was found which enables a more detailed understanding of the chemical nature of these systems. In order to examine the oxygen sensitivity of $Fe^{II}-$ligand complexes, we preferred not to perform detailed quantitative kinetic measurements, due to the complex nature and demanding analysis of the multistep reactions between $[Fe^{II}(L)_x]$ and O_2.[43−46] However, it was as a first approximation sufficient to obtain a set of qualitative data, on which basis the different complexes could be compared. We could realize such a comparison by simply introducing air into solutions of $[Fe^{II}(L)_x]$ complexes and recording UV/Vis spectra before and during the bubbling period in time sequences of 1, 3, 5, 10, 15, 30, 60 ... minutes. The degree of oxidation could easily be followed by the increase in absorbance below 400 nm. The time in which more than approx. 80% of the $[Fe^{II}(L)_x]$ complex was converted into the $[Fe^{III}(L)_x]$ complex was taken as "qualitative oxidation time" and entered for comparison purposes in the qualitative time scale of Figure 8**b**. It can be seen from

Figure 8**b** that the range of "qualitative oxidation time" varies from the totally inert hexaaqua complex to the extremely oxygen sensitive complexes of EDTA, 1,2-PDTA, which are oxidized within a few seconds and can no more be determined accurately by this qualitative method.

A good correlation exists between the oxygen sensitivity of $[Fe^{II}(L)_x]$ complexes and the stability constants of their nitrosyl complexes, which is clearly seen from the comparison in Figure 8**a** and 8**b**. In general, the higher the K_{NO} value for the nitrosyl complex, the shorter the "qualitative oxidation time". Obviously, an increasing inductive effect of the chelate ligand causes both an increasing stability of the $Fe^{II}-NO$ bond in the nitrosyl complexes, and also an enhanced electron transfer from Fe^{II} to O_2 in the corresponding $[Fe^{II}(L)_x]$ complexes. The two extreme cases are on the one hand "naked" $[Fe^{II}(H_2O)_6]^{2+}$ with its very low affinity for both dioxygen and NO, and on the other hand the $[Fe^{II}(EDTA)]^{2-}$ complex with its very high affinity for both dioxygen and NO. Thus the stability of the Fe(L)NO complex directly correlates with the oxygen sensitivity of the $Fe^{II}(L)$ complex, i.e. with the ability to form $Fe^{III}-O_2^-$. This again suggests that the stability of the Fe(L)NO complex is also controlled by its ability to bind NO as $Fe^{III}-NO^-$, which correlates with the position of the *LMCT* band observed in Figure 9. These trends should then also correlate with the redox potentials of the $Fe^{II/III}(L)$ complexes (see Table 3).

Table 3. Redox potentials vs. NHE

$[Fe^{III}(H_2O)_6]^{3+}/[Fe^{II}(H_2O)_6]^{2+}$	$E_{1/2} = 0.771$ V	(ref.[47])
$[Fe^{III}(1,3\text{-PDTA})]^-/[Fe^{II}(1,3\text{-pdta})]^{2-}$	$E_{1/2} = 0.309$ V	(this work)
$[Fe^{III}(EDTA)]^-/[Fe^{II}(EDTA)]^{2-}$	$E_{1/2} = 0.129$ V	(this work)
$[Fe^{III}(DTPA)]^-/[Fe^{II}(DTPA)]^{2-}$	$E_{1/2} = 0.110$ V	(ref.[48])

It is seen from the quoted values that the tendency of $Fe^{II}(L)$ to be oxidized (as reflected by the lower redox potential) correlates directly with the oxygen sensitivity of $Fe^{II}(L)$ and its ability to bind NO. In these cases $Fe^{II}(L)$ is formally oxidized to effectively bind O_2 and NO as $Fe^{III}-O_2^-$ and $Fe^{III}-NO^-$, respectively.

Conclusion

The results reported in this study clearly demonstrate that the correlation found between the oxygen sensitivity and the K_{NO} values for the investigated complexes, makes it very difficult to find suitable $[Fe^{II}(L)_x]$ complexes that will show a low oxygen sensitivity and a high affinity to bind NO (i.e. $K_{NO} > 1\cdot10^6$ M^{-1}). The exceptionally high K_{NO} value for the HEDTRA complex and the more favorable relation between the oxygen sensitivity and K_{NO} values for the DTPA, CEIDA, and β-EDDADP complexes, suggest that these ligands are promising candidates for technical applications. However, so far no kinetic details are available, and the conclusions are based on thermodynamic stability constants for the binding of NO and qualitative observations on the oxygen sensitivity of the complexes. A detailed kinetic analysis of the "on" and "off" reactions for the interaction of $Fe^{II}(L)$ with NO is presently underway[46] and may reveal significant differences that will enable a kinetic control and further tuning of the overall process.

Experimental Section

General Remarks: All experiments were performed under strict exclusion of air oxygen. Buffer solutions were deaerated for extended periods (in general 1 minute per mL solution) with pure N_2 or Ar, or in some cases freeze-thaw cycles were performed under vacuum in order to completely remove the dissolved dioxygen in solution, before they were brought in contact with Fe^{II} salts or nitric oxide.

NO gas, purchased from Messer Griesheim or Rießner Gase in a purity of at least 99.5 vol%, was cleaned from trace amounts of higher nitrogen oxides like N_2O_3 and NO_2 by passing it through an Ascarite II column (NaOH on silica gel, Sigma–Aldrich). NO from a gas tank should not be used after six months following the date of its industrial preparation, since decomposition causes a drastic decrease in the purity of the gas. The decomposition is pressure dependent, which led us to only use bottles filled with a maximum pressure of 20 bar, and resulted in a longer life-time of the NO gas.

The chelate ligands AIDA, ATMP, BADA, 1,4-BDTA, ^{t}BIDA, DTPMP, *rac.* EDDS, (*s,s*)-EDDS,[49] EDG, EDTMP, EIDA, HPDTA, HPIDA, MIDA, NTA, 1,3-PDTA, and SMIDA were supplied by Akzo Nobel. All other ligands and chemicals were purchased from Arcos Chimica, Fluka, Lancaster Synthesis, or Sigma–Aldrich with the highest available purity (at least 97%). APTA was synthesized according to a procedure described in the literature.[50]

UV/Vis spectra were recorded on a Cary 1G UV/Vis spectrophotometer from Varian using a 1 cm quartz cuvette directly attached to a round flask with a sideway gas connection. This enabled the performance of different physical or chemical operations, like bubbling the solution with NO or N_2, and the measurement of spectra under exclusion of dioxygen in the same vessel.

IR spectra were recorded with the use of a two mirror ATR cell on a ATI Mattson FTIR *Infinity* spectrophotometer. The reflection instrument utilizes a Ge crystal as an internal reflection plate with a size of 50 × 20 × 2 mm and 45° angle of incidence. For each complex two independent measurements of 100 scans were performed under inert gas atmosphere.

The concentration of free nitric oxide in solution was determined with an ISO-NOP electrode connected to an ISO-NO Mark II nitric oxide sensor from World Precision Instruments. The NO electrode consists of a membrane covered anode which selectively oxidizes NO to NO_3^- ions. The resulting current is proportional to the concentration of NO in solution. The NO electrode was calibrated daily with fresh solutions of sodium nitrite and potassium iodide according to the method suggested by the manufacturers. The calibration factor nA/μM was determined with a linear fit program.

Potentiometric measurements were performed on a METROHM 702 SM Titrino in a jacketed, air-tight glass titration cell equipped with a combined pH glass electrode (METROHM 6.0203.100), N_2 inlet and outlet, and a graduated 10 mL microburet (METROHM 6.1518.210). The electrode was calibrated with strong acid and strong base so as to read directly in hydrogen ion concentration.

The ion product of water, i.e. $pK_W = -\log[H^+][OH^-] = 13.85$, was determined experimentally. A carbonate-free 0.10 M sodium hydroxide solution was prepared with boiled distilled water and was standardized by titrations with potassium hydrogen phthalate. Gran's method[51] was used to confirm the absence of carbonate in the sodium hydroxide standard solution. The NaOH solution was stored under nitrogen. All solutions were adjusted to an ionic strength of 0.5 M with $NaClO_4$. The temperature was maintained at 25.0 ± 0.1 °C by circulating thermostated water through the outer jacket of the cell. All measurements were carried out while bubbling N_2 through the solution.

pH measurements were performed with the aid of a Mettler Delta 340 pH-meter. The reference electrode was filled with NaCl instead of KCl to prevent precipitation of $KClO_4$.

Cyclic voltammogramms were recorded with an EG&G PARC potentiostat-galvanostat Model 263 controlled by a PC. The electrochemical cell was a conventional one with three electrodes. The reference electrode was Ag/AgCl, the counter electrode was a platinum sheet and a glassy carbon electrode was used as the working electrode (all from BAS). Solutions for cyclic voltammetry were fully deoxygenated with nitrogen for at least 1 h. Following deoxygenation, the behavior of the electrode was studied in the buffer solution and checked by measurements on the redox couple of $K_3[Fe(CN)_6]$. Reported $E_{1/2}$ values are corrected to the NHE scale. The concentration of the solutions was 5 mM for $[Fe^{II}(EDTA)]^{2-}$ and $[Fe^{II}(1,3\text{-PDTA})]^{2-}$. Solutions were prepared by dissolving the respective ligand and $Fe_2(SO_4)_3 \cdot 5\,H_2O$ in 0.1 M acetate buffer at pH 5. The ionic strength was adjusted to 0.5 M ($NaClO_4$).

In all UV/Vis experiments, solutions of 1 mM of Fe^{II} chelates in 100 mM acetate buffer at pH 5.0 were used. The Fe^{II} complexes were prepared from $FeSO_4 \cdot 7\,H_2O$ and the chelate in an excess of 10 to 50% over the required stoichiometric amount, i.e. between 1.1 and 1.5 mM in the case of the EDTA analogues, and between 2.2 and 3.0 mM in the case of the MIDA analogues. In each buffer solution the ionic strength was adjusted to a value of 0.5 M by addition of calculated amounts of sodium perchlorate. For ATR-IR measurements, unbuffered solutions of Fe^{II} chelates at a concentration of up to 200 mM were used.

Acknowledgments

The authors gratefully acknowledge financial support from Akzo Nobel Functional Chemicals, Paques Bio Systems, Fonds der Chemischen Industrie and the Max-Buchner-Forschungsstiftung.

[1] S. G. Chang, D. Littlejohn, S. Lynn, *Environ. Sci. Technol.* **1983**, *17*, 649.
[2] W. Weisweiler, B. Retzlaff, L. Raible, *Chem. Eng. Proc.* **1984**, *18*, 85.
[3] E. Sada, H. Kumazawa, Y. Takada, *Ind. Eng. Chem. Fundam.* **1984**, *23*, 60.
[4] E. Sada, H. Kumazawa, H. Hikosaka, *Ind. Eng. Chem. Fundam.* **1986**, *25*, 386.
[5] E. Sada, H. Kumazawa, H. Machida, *Ind. Eng. Chem. Res.* **1987**, *26*, 2016.
[6] S. S. Tsai, S. A. Bedell, L. H. Kirby, D. J. Zabick, *Environ. Prog.* **1989**, *8*, 126.
[7] V. Zang, R. van Eldik, *Dechema-Monographien* **1989**, *118*, 143.
[8] P. Harriott, K. Smith, L. B. Benson, *Environ. Prog.* **1993**, *12*, 110.
[9] E. K. Pham, S. G. Chang, *Nature* **1994**, *369*, 139.
[10] Y. Hishinuma, R. Kaji, H. Akimoto, F. Nakajima, T. Mori, T. Kamo, Y. Arikawa, S. Nozawa, *Bull. Chem. Soc. Jpn.* **1979**, *52*, 2863.
[11] D. Littlejohn, S. G. Chang, *J. Phys. Chem.* **1982**, *86*, 537.
[12] N. Lin, D. Littlejohn, S. G. Chang, *Ind. Chem. Proc. Des. Dev.* **1982**, *21*, 725.
[13] 1. M. S. Ward and R. E. Shepherd, *Inorg. Chim. Acta* **1999**, *286*, 197.
[14] R. E. Shepherd, M. A. Sweetland, D. E. Junker, *J. Inorg. Biochem.* **1997**, *65(1)*, 1.
[15] [15a] T. Mizuta, J. Wang, K. Miyoshi, *Bull. Chem. Soc. Jpn.* **1993**, *66*, 2547. – [15b] T. Mizuta, J. Wang, K. Miyoshi, *Inorg. Chim. Acta* **1995**, *230*, 119.
[16] J. F. Demmink, I. C. F. van Gils, A. A. C. M. Beenackers, *Ind. Eng. Chem. Res.* **1997**, *36*, 4914 and cit. lit.
[17] V. Zang, M. Kotowski, R. van Eldik, *Inorg. Chem.* **1988**, *27*, 3279.
[18] V. Zang, R. van Eldik, *Inorg. Chem.* **1990**, *29*, 4462.
[19] G. Schwarzenbach, G. Anderegg, W. Schneider, H. Senn, *Helvetia Chim. Acta* **1955**, *132*, 1147.
[20] [20a] L. Zélány, I. Nagypál, G. Peintler, *PSEQUAD*, L. Kossuth University of Debrecen, **1983**; – [20b] L. Zélány, I. Nagypál, *Computational Methods for the Determination of Formation Constants*, Plenum Press, New York, **1985**.
[21] R. M. Smith, A. E. Martell, *Critical Stability Constants*, No. 6, Plenum Press, New York, **1989.**
[22] K. J. Powell, *Soleq: Mini-SCDatabase*, Academic Software, **1999**.
[23] T. Schneppensieper, A. Zahl, R. van Eldik, unpublished results.
[24] C. A. Brown, M. A. Pavlosky, T. E. Westre, Y. Zhang, B. Hedman, K. O. Hodgson, E. I. Solomon, *J. Am. Chem. Soc.* **1995**, *117*, 715.
[25] J. A. McCleverty, *Chem. Rev.* **1979**, *79*, 53.
[26] K. Ogura, M. Watanabe, *Electrochim. Acta* **1982**, *27*, 111.
[27] R. J. P. Williams, *Chem. Soc. Rev.* **1996**, *25*, 77.
[28] C. Hauser, T. Glaser, E. Bill, T. Weyhermüller, K. Wieghardt, *J. Am. Chem. Soc.* **2000**, *122*, 4352.
[29] P. Lainé, A. Gourdon, J.-P. Launey, *Inorg. Chem.* **1995**, *34*, 5129.
[30] P. Lainé, A. Gourdon, J.-P. Launey, *Inorg. Chem.* **1995**, *34*, 5138.
[31] P. Lainé, A. Gourdon, J.-P. Launey, J.-P. Tuchagues, *Inorg. Chem.* **1995**, *34*, 5150.
[32] P. Lainé, A. Gourdon, J.-P. Launey, *Inorg. Chem.* **1995**, *34*, 5156.
[33] D. M. P. Mingos, D. J. Sherman, *Adv. Inorg. Chem.* **1989**, *34*, 293.
[34] J. S. Stamler, D. J. Singel, J. Loscalzo, *Science* **1992**, *258*, 1898.
[35] Y.-M. Chiou, L. Jr. Que, *Inorg. Chem.* **1995**, *34*, 3270.
[36] R. G. J. Miller, B. C. Stace, *Laboratory Methods in Infrared Spectroscopy, Hayden, London* **1972**, *Chapter 14*, 205.
[37] V. Zang, Dissertation, Universität Witten-Herdecke **1990**.
[38] Y. Kurimura, R. Ochiai, N. Matsuura, *Bull. Chem. Soc. Jpn.* **1968**, *41*, 2234.
[39] T. Schneppensieper, Diplomarbeit, Universität Erlangen-Nürnberg **1997**.
[40] E. Sada, H. Kumazawa, H. Machida, *Ind. Eng. Chem. Res.* **1987**, *26*, 1468.
[41] V. Zang, R. van Eldik, *Inorg. Chem.* **1990**, *29*, 1705.
[42] H. J. Wubs, A. A. C. M. Beenackers, *Ind. Eng. Chem. Res.* **1993**, *32*, 2580.
[43] S. Seibig, R. van Eldik, *Inorg. Chem.* **1997**, *36*, 4115.
[44] S. Kudo, J. L. Bourassa, S. E. Boggs, Y. Sato, P. C. Ford, *Anal. Biochem.* **1997**, *247*, 193.
[45] I. Cebulla, Dissertation, Universität Tübingen **1995**.
[46] A. Wanat, T. Schneppensieper, R. van Eldik, unpublished results.
[47] J. Burgess, *Ions in Solution*, Ellis Horwood Series In Inorganic Chemistry, New York, **1988**.
[48] E. R. Brown, J. D. Mazzarella, *J. Electroanal. Chem.* **1987**, *222*, 173.
[49] N. Zwicker, *GIT-Labor-Fachzeitschrift* **1999**, *10*, 1044.
[50] Z. Hualin, L. Peiyi, W. Boyi, W. Jianhua, Z. Peiju, *Polyhedron* **1990**, *9*, 2873.
[51] G. Gran, *Analyst* **1952**, *77*, 661.

Received May 23, 2000
[I00210]